

# Support for Non-conformal Meshes in PETSc’s DMPlex Interface

TOBIN ISAAC, The University of Chicago  
MATTHEW G. KNEPLEY, Rice University

A

PETSc’s DMPlex interface for unstructured meshes has been extended to support non-conformal meshes. The topological construct that DMPlex implements—the CW-complex—is by definition conformal, so representing non-conformal meshes in a way that hides complexity requires careful attention to the interface between DMPlex and numerical methods such as the finite element method. Our approach—which combines a tree structure for subset-superset relationships and a “reference tree” describing the types of non-conformal interfaces—allows finite element code written for conformal meshes to extend automatically: in particular, all “hanging-node” constraint calculations are handled behind the scenes. We give example code demonstrating the use of this extension, and use it to convert forests of quadtrees and forests of octrees from the p4est library to DMPlex meshes.

Additional Key Words and Phrases: unstructured meshes, non-conformal meshes, adaptive mesh refinement, quadtrees, octrees

## ACM Reference Format:

Tobin Isaac and Matthew G. Knepley, 2015. Support for Non-conformal Meshes in PETSc’s DMPlex Interface. *ACM Trans. Math. Softw.* V, N, Article A (January YYYY), 16 pages.  
DOI: <http://dx.doi.org/10.1145/0000000.0000000>

## 1. INTRODUCTION

PETSc [Balay et al. 2015a; Balay et al. 2015b] is an actively developed and widely used library for numerical methods in scientific computing, providing parallel data management, structured and unstructured meshes, linear and nonlinear algebraic solvers and preconditioners, time integrators and optimization algorithms. Many of these methods (such as geometric multigrid and domain decomposition linear and nonlinear solvers) can take advantage of the geometric/topological setting of a discretized problem, i.e. mesh information. PETSc’s interface for serving mesh data to numerical algorithms is the **DM** object. PETSc has native DM implementations for several mesh formats, and implementations that wrap external libraries may also be registered, such as **DM-MOAB** for MOAB [Tautges et al. 2004]. Because of PETSc’s pointer-to-implementation approach to method extensibility, external implementations may cover only those methods in the DM API that are necessary for their target applications. While no DM implementation is privileged above others—PETSc-native and external implementations are registered in the same way—the native implementations of structured grids (**DMDA**) and unstructured meshes (**DMPlex**) have the most complete coverage of the DM API, and are developed most actively. Only DMPlex, for example, currently has complete support for the **PetscFE** and **PetscFV** implementations of the finite element method and finite volume method.

Many mesh formats lie between structured grids and unstructured meshes and can broadly be described as hierarchical mesh formats. Examples include red-green refinement of triangular meshes, quadtree/octree refinement of quadrilateral/hexahedral meshes, and nested Cartesian grids. These formats are often implemented in frameworks with data structures that are advantageous for certain data access patterns. Patch-based nested grids, for instance, are optimized for fast stencil operations. Another example is red-green refined triangular meshes, where the triangles have been ordered by a

---

Permission to make digital or hard copies of all or part of this work for personal or classroom use is granted without fee provided that copies are not made or distributed for profit or commercial advantage and that copies bear this notice and the full citation on the first page. Copyrights for components of this work owned by others than ACM must be honored. Abstracting with credit is permitted. To copy otherwise, or republish, to post on servers or to redistribute to lists, requires prior specific permission and/or a fee. Request permissions from [permissions@acm.org](mailto:permissions@acm.org).  
© YYYY ACM. 0098-3500/YYYY/01-ARTA \$15.00  
DOI: <http://dx.doi.org/10.1145/0000000.0000000>

Sierpinski curve: these meshes can efficiently compute residuals of discontinuous-Galerkin or finite volume operators without explicitly determining which cells are adjacent to each-other by pushing fluxes onto stacks [Bader et al. 2012].

We would like to be able to convert hierarchical mesh formats into the DMPlex unstructured format. Our main reason is that the efficiency gains of hierarchical mesh formats typically come at the expense of flexibility and generality. DMPlex supports, for instance, arbitrary mesh partitions and the extraction of arbitrary subsets of cells (or facets) as submeshes: features which are typically missing from hierarchical meshing frameworks. The broad support of DMPlex for PETSc’s DM API also makes it an ideal format for testing and comparing numerical methods that call on the DM interface.

What has prevented the conversion of these meshes in the past is that hierarchical meshes are often non-conformal meshes: this is true of quadtrees, octrees, nested Cartesian grids, and of some hierarchical simplicial meshes as well. CW-complexes—the topologies DMPlex was designed to represent—are by definition conformal. Our recent extension of DMPlex has addressed this short-coming. In this paper we describe how we represent non-conformal hierarchical meshes in DMPlex in a way that minimally disturbs the way DMPlex interacts with the other components of PETSc, and that requires minimal input from the user.

## 2. PRELIMINARIES: CONFORMAL MESHES

We begin with a brief review of the DMPlex interface and the finite element method in the context of conformal meshes.

### 2.1. CW-complexes and DMPlex

The triangulation of a domain  $\Omega$  into cells generates a CW-complex (see, e.g., [Hatcher 2002, Chapter 10]). In short, a CW-complex is a partition of a  $d$ -dimensional spaces into well-shaped open cells with dimensions between 0 and  $d$ , such that the boundary of each  $n$ -cell ( $n > 0$ ) is partitioned by finitely many lower-dimensional cells. We call cells of every dimension “points” in the complex.

In a CW-complex, the basic relationship that defines the topology is the map from an  $n$ -cell  $A$  to the  $(n - 1)$ -cells on its boundary, which we call the cone of  $A$ ,  $\text{cone}(A)$ , following the terminology in [Knepley and Karpeev 2009]. The closure of the cone map,

$$\text{clos}(A) := \{A\} \cup \text{cone}(A) \cup \text{cone}(\text{cone}(A)) \cup \dots, \quad (1)$$

corresponds to closure in  $\bar{\Omega}$ , i.e.,  $\text{clos}(A)$  partitions  $\bar{A}$ .

The reverse map, taking the  $n$ -cell  $A$  to its adjacent  $(n + 1)$ -cells, is called the support map,  $\text{supp}(A)$ , and the closure of the support map is called the star of  $A$ ,  $\text{star}(A)$ . It is important to note at this point that for conformal meshes, cones and supports are dual,

$$B \in \text{clos}(A) \Leftrightarrow A \in \text{supp}(B). \quad (2)$$

A CW-complex can be represented by a Hasse diagram for stratified partially-ordered sets: the depth of a stratum corresponds to the topological dimension of its points, upward arrows represent cone maps, and downward arrows represent support maps. These concepts (cones, supports, strata) are at the core of the DMPlex interface, which we illustrate in Figs. 1 to 5.

### 2.2. The reference element and element maps

We assume a Ciarlet reference finite element  $(\hat{K}, P(\hat{K}), \hat{\Sigma})$  (reference cell, space, and dual basis) is specified and a domain  $\Omega$  is triangulated into a mesh of  $N_K$  cells, with cell  $K_i$  being the image of  $\hat{K}$  under a smooth embedding  $\varphi_i : \hat{K} \rightarrow \bar{\Omega}$ . A finite-dimensional subspace  $V_h$  of a function space  $V(\Omega)$  is then specified as the set of functions  $v \in V$  such that the pullback  $\varphi_i^* v := v \circ \varphi_i$  is in  $P(\hat{K})$  for each  $\varphi_i$ . (Discretizations of  $H^{\text{curl}}(\Omega)$ - and  $H^{\text{div}}(\Omega)$ -conforming spaces are often pulled back onto reference

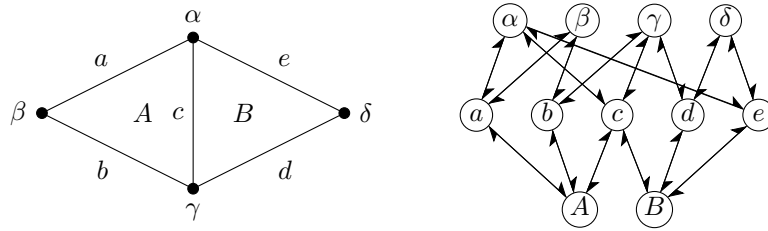


Fig. 1. A two-triangle mesh and its Hasse diagram.

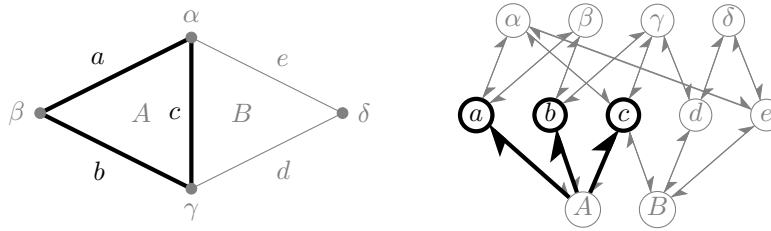


Fig. 2.  $\text{cone}(A)$  /  $\text{DMplexGetCone}()$ .

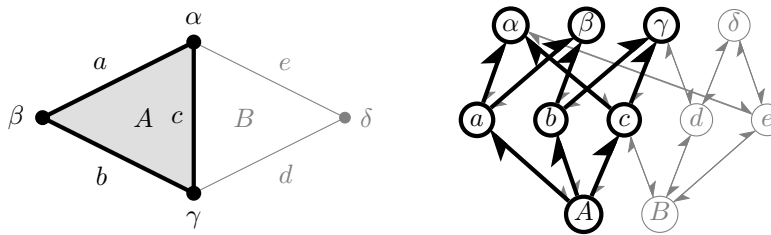


Fig. 3.  $\text{clos}(A)$  /  $\text{DMplexGetTransitiveClosure}(\text{useCone}=\text{PETSC\_TRUE})$ .

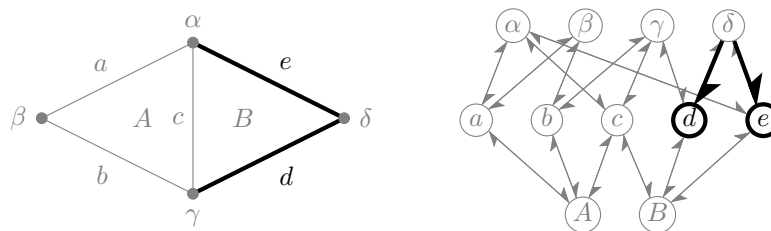


Fig. 4.  $\text{supp}(\delta)$  /  $\text{DMplexGetSupport}()$ .

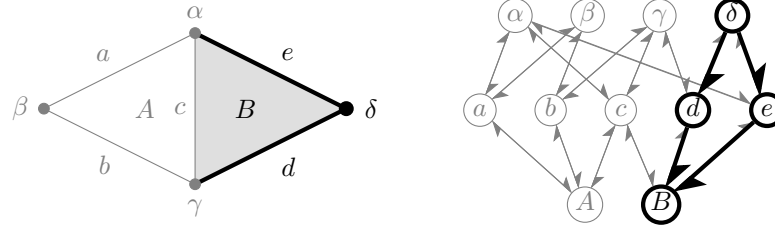
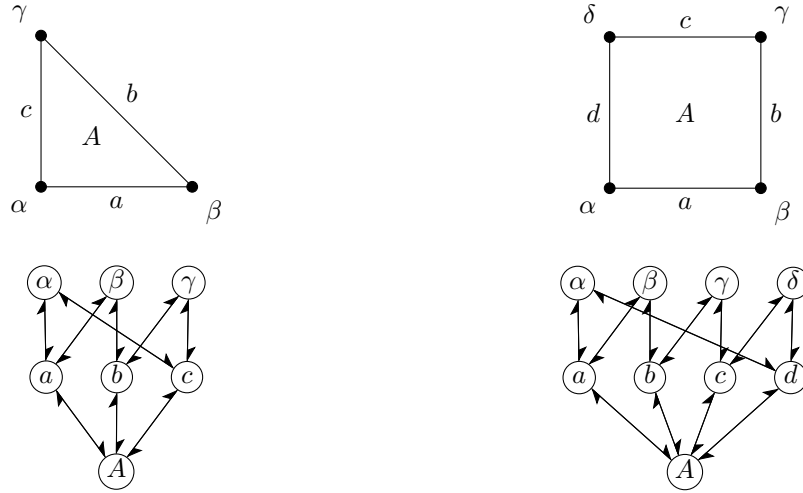
Fig. 5.  $\text{star}(\delta) / \text{DMPlexGetTransitiveClosure}(\text{useCone}=\text{PETSC\_FALSE})$ .

Fig. 6. The reference triangle, reference quadrilateral, and the Hasse diagrams of their CW-complexes.

elements using covariant and contravariant Piola transformations, which have minor implications discussed Section 6.1.) The adjoint of the pullback is the pushforward  $(\varphi_{i*}\sigma)(v) := \sigma(\varphi_i^*v)$ : it pushes  $\hat{\Sigma}$  forward onto a set of functionals in  $V_h^*$ ,

$$\Sigma_i := \varphi_{i*}\hat{\Sigma}. \quad (3)$$

To the conventional triplet  $(\hat{K}, P(\hat{K}), \hat{\Sigma})$ , we add a reference CW-complex  $\hat{S}$ , which decomposes the closure of  $\hat{K}$  (Fig. 6).

### 2.3. The finite element method for conformal meshes in DMPlex

We now list three assumptions that are implicit in most finite element discretizations for conformal meshes, and thus in the data structures and functions that DMPlex uses to implement the finite element method. Making these typically implicit assumptions explicit will help to explain the extension of DMPlex to non-conformal meshes in Section 3.

First, we assume that the reference complex  $\hat{S}$  also decomposes the dual basis  $\hat{\Sigma}$ , in that the shape function associated with each  $\sigma \in \hat{\Sigma}$  is supported in the star of a point in  $\hat{S}$ . We formalize this as assumption I.

I. For each  $\sigma_k \in \hat{\Sigma}$  there is a point  $p \in \hat{S}$  such that, if  $\psi_k \in P(\hat{K})$  is  $\sigma_k$ 's shape function ( $\sigma_j(\psi_k) = \delta_{jk}$ ), then  $\text{supp}(\psi_k) = \cup \text{star}(p)$ .

Assumption I is satisfied by essentially all finite elements: it allows for the definition of compactly supported basis functions of  $V_h$ . We will refer to the reference functionals associated with  $p \in \hat{S}$  as  $\hat{\Sigma}^p$ , so that  $\hat{\Sigma} = \cup_{p \in \hat{S}} \hat{\Sigma}^p$ , and to the pushforward of those functionals under  $\varphi_i$  as  $\Sigma_i^p := \varphi_{i*} \hat{\Sigma}^p$ , so that  $\Sigma_i = \cup_{p \in \hat{S}} \Sigma_i^p$ .

Second, we assume that the embeddings of neighboring cells are compatible, in that the traces of their approximation spaces “line up” so that  $H^1(\Omega)$  functions can be constructed, which we formalize as assumption II.

II. If  $C := \overline{K_i} \cap \overline{K_j} \neq \emptyset$ , then  $\psi \in P(\varphi_j^{-1}(C)) \Rightarrow \varphi_i^* \varphi_j^{-*} \psi \in P(\varphi_i^{-1}(C))$  (where  $\varphi_j^{-*} := (\varphi_j^*)^{-1}$  and  $P(X)$  is the trace space of  $P(\hat{K})$  on  $X \subset \overline{\hat{K}}$ ).

Finally, we assume that the dual bases of adjacent cells are compatible, in that the mappings of adjacent cells push functionals forward on top of each other, which we formalize as assumption III.

III. If  $p, q \in \hat{S}$  and there are adjacent cells  $K_i$  and  $K_j$  such that  $\varphi_i(p) = \varphi_j(q)$ , then there is a permutation  $M$  such that  $\Sigma_i^p = M \Sigma_j^q$ .

The permutations typically encode the symmetries of the polytopes in  $\hat{S}$ , e.g., reversal for edges, and dihedral symmetries for faces.

For each vector  $v \in V_h$  and each element  $K_i$ , we need to be able to evaluate  $\Sigma_i(v)$ . Given a choice of basis  $W$  for  $V_h^*$ , each element has a *restriction matrix*  $R_i$  such that  $\Sigma_i(v) = R_i W(v)$ . For a conformal mesh, assumptions I, II, and III allow for a *global nodal basis* to be defined for  $V_h^*$ : a basis  $W$  that is the union of the pushforward dual bases,

$$W := \cup_{i=1}^{N_K} \cup_{p \in \hat{S}} \Sigma_i^p. \quad (4)$$

We may also think of  $W$  as being decomposed into the functional associated with points in  $S$ ,

$$W = \cup_{s \in S} \Sigma^s, \quad (5)$$

where  $\Sigma^s := \Sigma_i^p$  (up to a permutation) if  $\varphi_i(p) = s$ . With a global nodal basis, the restriction matrix  $R_i$  for each cell  $K_i$  is a binary matrix, and there is a subset  $W_i$  of  $W$  such that  $\Sigma_i = R_i W = W_i$ .

Here we see the utility of representing a conformal mesh as a CW-complex  $S$ . Given a map  $G : S \rightarrow 2^W$  from each point in  $S$  to its set of associated functionals in  $W$ , we can compute  $W_i$  as  $G(\text{clos}(K_i))$ , since  $\text{clos}(K_i)$  is the image of the reference complex  $\hat{S}$  under  $\varphi_i$ .

In DMPlex, the map  $G$  is represented by a **PetscSection**. For a typical finite element, the number of functionals associated with a point  $p \in S$  is a function only of  $p$ 's topological dimension, so that  $G$  can be calculated purely from the sizes of the strata of  $S$ : if a DMPlex has been given a finite element object (PetscFE), it constructs  $G$  automatically, and makes it available by **DMGetDefaultGlobalSection()**. The set  $\text{clos}(K_i)$  can be constructed with **DMPlexGetTransitiveClosure()**, which is used to construct  $\Sigma_i(v)$  on a vector  $v \in V_h^*$  in the function **DMPlexVecGetClosure()**. This function is called within tight, performance critical loops when computing residuals or calculating Jacobians (which we illustrate in a prototypical residual evaluation function in Ex. 1), so when considering representations of non-conformal meshes in DMPlex, we chose to avoid those that would require modifications at this level of granularity.

### 3. NON-CONFORMAL MESHES

In this section we describe the way non-conformal meshes can now be represented in DMPlex, and we describe a general approach to computing with finite elements on these meshes.

**EXAMPLE 1:** finite element residual  $\mathbf{r} = f(\mathbf{v})$  using DMPlex ( $\mathbf{dm}$ )

---

```

1 PetscInt c, cSize, cStart, cEnd;
2 Vec      vLocal, rLocal;

   /* Get vectors for the local representations */
3 DMGetLocalVector(dm,&vLocal);
4 DMGetLocalVector(dm,&rLocal);
   /* Get the support of v on the local subdomain of this MPI process */
5 DMGlobalToLocalBegin(dm,v,INSERT_VALUES,vLocal);
6 DMGlobalToLocalEnd  (dm,v,INSERT_VALUES,vLocal);
   /* Get the range of cell indices (cells are the lowest stratum) */
7 DMPlexGetHeightStratum(dm,0,&cStart,&cEnd);
8 if (cEnd > cStart) {
9     PetscScalar *vElem, *rElem;
   /* Get the size of the element dual space  $\hat{\Sigma}$  */
10  DMPlexGetVecClosure(dm,NULL,vLocal,cStart,&cSize,NULL);
   /* Get workspace arrays */
11  DMPlexGetWorkArray(dm,cSize,PETSC_SCALAR,&vElem);
12  DMPlexGetWorkArray(dm,cSize,PETSC_SCALAR,&rElem);
   /* Compute the local residual */
13  VecSet(rLocal,0.0);
14  for (c = cStart; c < cEnd; c++) {
   /* Get the restriction of v to cell c */
15  DMPlexVecGetClosure(dm,NULL,vLocal,c,&cSize,&vElem);
   /* Compute the element contribution to the residual */
   /* ... [rElem = f(vElem)] */
   /* Sum the element residual into the local residual vector */
16  DMPlexVecSetClosure(dm,NULL,rLocal,c,rElem,ADD_VALUES);
17  }
   /* Free workspace */
18  DMPlexRestoreWorkArray(dm,cSize,PETSC_SCALAR,&vElem);
19  DMPlexRestoreWorkArray(dm,cSize,PETSC_SCALAR,&rElem);
20 }
   /* Sum process contributions into r */
21 VecSet(r,0.0);
22 DMLocalToGlobalBegin(dm,rLocal,ADD_VALUES,r);
23 DMLocalToGlobalEnd  (dm,rLocal,ADD_VALUES,r);
   /* Free local vectors */
24 DMRestoreLocalVector(dm,&vLocal);
25 DMRestoreLocalVector(dm,&rLocal);

```

---

**3.1. Representing non-conformal meshes in DMPlex**

The representation of non-conformal meshes that has been added to DMPlex is limited to hierarchical non-conformal meshes. By hierarchical we mean that two mesh points  $p, q \in S$  overlap only if one is a superset of the other,

$$(p \cap q \neq \emptyset) \Rightarrow ((p \subseteq q) \vee (q \subseteq p)). \quad (6)$$

Constructing function spaces on non-conformal meshes that are not hierarchical is more complicated, and not considered here.

In Fig. 7 we show a simple three-triangle mesh with a non-conformal interface between triangle  $A$  on one side and triangles  $B$  and  $C$  on the other, and we have also labeled all of the edges and

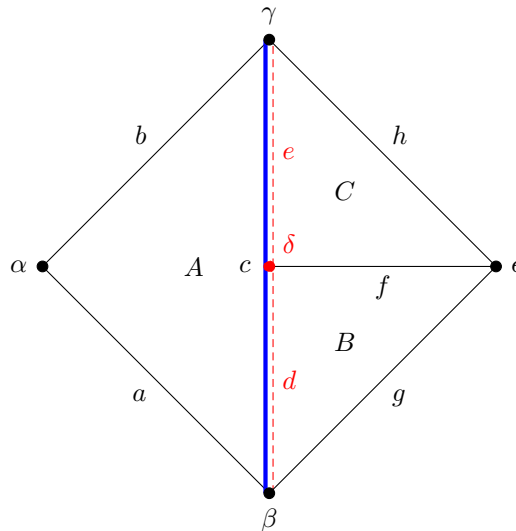


Fig. 7. A simple non-conformal mesh.

vertices of the triangles. The question when representing this mesh in DMPlex is how to treat the edge  $c$  and the edges  $d$ ,  $e$ , and vertex  $\delta$  that overlap it.

The only way to represent this mesh as a true CW-complex (which cannot have overlapping points) is to remove the long edge  $c$  (Fig. 8), but then the cell  $A$  would not be considered a triangle: it would be considered a degenerate quadrilateral, with  $d$  and  $e$  in the cone of  $A$ . This is a poor format for finite element computations for two reasons. The first is that the support of a basis function is no longer correlated with the star operator. A hat function centered at vertex  $\gamma$ , for instance, is non-zero on cell  $B$ , but  $B \notin \text{star}(\gamma)$ . The second reason is that the shape of  $\text{clos}(A)$  is not the same as for other triangles, so `DMPlexVecGetClosure()` would require special handling to restrict a function to  $A$ .

Given these considerations, we include both super-points and sub-points (or “parents” and “children” henceforth) in the representations of non-conformal meshes in DMPlex. In addition, we make the following extensions to the format, illustrated in Fig. 9:

- (1) We add to the Hasse diagram, which is traversed with `cone()` and `supp()` operations, a separate tree structure, which is traversed with `parent()` and `children()` operations (in DMPlex, `DMPlexGetTreeParent()` and `DMPlexGetTreeChildren()`).
- (2) We break the duality between `cone()` and `supp()` operations. In particular, the cone of an  $n$ -cell  $p$  includes the “natural” decomposition of its boundary into  $(n - 1)$ -cells (e.g., the three edges of a triangle), while the support of  $p$  is the set of  $(n + 1)$ -cells whose boundaries intersect  $p$ . It is still the case that  $q \in \text{cone}(p) \Rightarrow p \in \text{supp}(q)$ , but the converse is not true for non-conformal meshes. In the mesh in Fig. 9, for example,  $A \in \text{supp}(d)$  because  $\partial A \cap d \neq \emptyset$ , but  $d \notin \text{cone}(A)$ , because it is not one of the canonical edges of  $A$ . The extra support maps are included because:
  - It ensures that  $\text{star}(p)$  covers the support of  $p$ 's basis functions, which is important for determining the sparsity pattern of finite element matrices (if  $\text{star}(p) \cap \text{star}(q) \neq \emptyset$ , then there may be non-zeros entries in a finite element matrix for their degrees of freedom).
  - It ensures that the support of a facet (a  $(d - 1)$ -dimensional cell) can be used to identify neighboring cells for finite volume and discontinuous Galerkin methods.





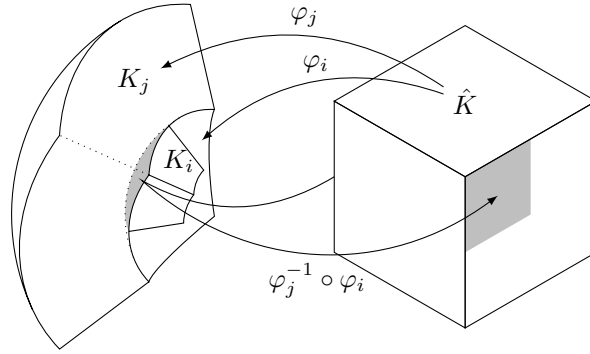


Fig. 10. Even though the embeddings  $\varphi_i$  and  $\varphi_j$  of  $K_i$  and  $K_j$  are curvilinear,  $\varphi_j^{-1} \circ \varphi_i$  is component-wise affine, so  $H^1(\Omega)$ -conforming spaces can be constructed from tensor-product polynomials on  $\hat{K}$ .

### 3.2. The finite element method for non-conformal meshes

For a non-conformal mesh, a global nodal basis as defined in the previous section is generally not possible: the union of all element functionals,

$$W^u := \cup_{i=1}^{N_K} \cup_{p \in \hat{S}} \Sigma_i^p, \quad (7)$$

will contain linear dependencies. For a hierarchically non-conformal mesh  $S$ , however, it is possible to construct a global basis  $W^c$  that is nearly nodal, by including only the functionals of points that have no ancestors,

$$W^c := \cup_{i=1}^{N_K} \cup \{p \in \hat{S} : \text{parent}(\varphi_i(p)) = \emptyset\} \Sigma_i^p. \quad (8)$$

There is then a *constraint matrix*  $I_c^u$  such that  $W^u(v) = I_c^u W^c(v)$  for all  $v \in V_h$ . These are sometimes referred to as “hanging-node” constraints. In this section, we describe the general method for calculating  $I_c^u$ .

We retain assumptions I, II, and III from Section 2 when considering non-conformal meshes. Assumption II—that neighboring approximations spaces “line up” for  $H^1(\Omega)$ -conforming constructions—limits the types of non-conformal interfaces that can occur. Given neighboring cells  $K_i$  and  $K_j$  and  $p, q \in \hat{S}$  such that  $\varphi_i(p) \subset \varphi_j(q)$ , then  $\varphi_i^* \varphi_j^{-*}$  must map  $P(\varphi_j^{-1} \varphi_i(p))$  onto  $P(p)$ . For simplicial elements with polynomial spaces, this typically means  $\varphi_j^{-1} \circ \varphi_i : p \rightarrow q$  is affine; for hypercube elements with tensor-product polynomial spaces,  $\varphi_j^{-1} \circ \varphi_i$  must be component-wise affine. We note that this is not a requirement that  $\varphi_i$  or  $\varphi_j$  be affine (Fig. 10).

When these conditions are met, we can expand each functional in  $\Sigma_i^p$  in terms of functionals in  $\Sigma_j$ : for each  $\sigma_r \in \hat{\Sigma}^p$ ,

$$(\varphi_{i*} \sigma_r)(v) = (\varphi_{i*} \sigma_r)(\varphi_j^{-*} \varphi_j^* v) \quad (9)$$

$$= (\varphi_{j*}^{-1} \varphi_{i*} \sigma_r)(\varphi_j^* v) \quad (10)$$

$$= \sum_{\sigma_s \in \hat{\Sigma}} (\varphi_{j*}^{-1} \varphi_{i*} \sigma_r)(\psi_s) \sigma_s(\varphi_j^* v) \quad (11)$$

$$= \sum_{\sigma_s \in \Sigma_j} (\varphi_{j*}^{-1} \varphi_{i*} \sigma_r)(\psi_s) \sigma_s(v), \quad (12)$$

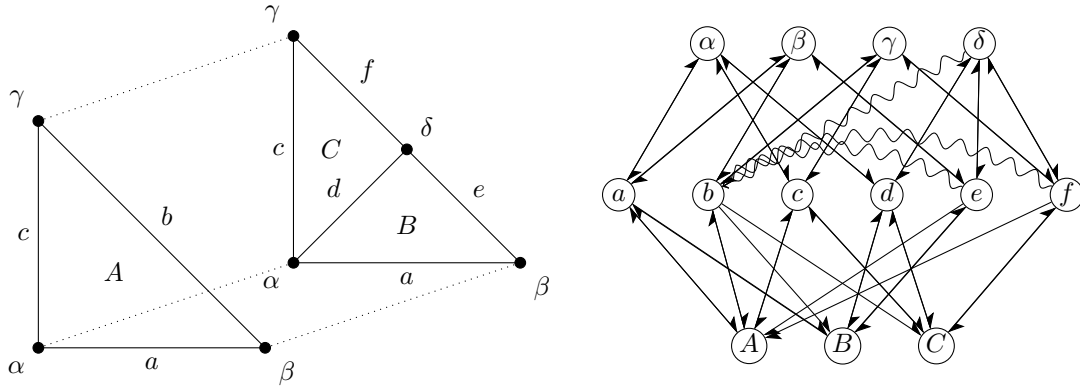


Fig. 11. The reference tree  $\hat{T}$  for red-green refinement of triangles. Notice that the reference element  $\hat{S}$  is included as a sub-complex of  $\hat{T}$ .

where  $\psi_s$  is again the shape function of  $\sigma_s$ . The transferred functional  $\varphi_{j*}^{-1}\varphi_{i*}\sigma_r$  can only be supported on  $q$ , so  $(\varphi_{j*}^{-1}\varphi_{i*}\sigma_r)(\psi_s) = 0$  if  $q \notin \text{supp}(\psi_s)$ . By assumption I, this means that the terms in Eq. (12) are non-zero only if  $\sigma_s \in \Sigma^t$  for  $t \in \text{clos}(\text{parent}(\varphi_i(p)))$ ,

$$(\varphi_{i*}\sigma_r)(v) = \sum_{\sigma_s \in \cup_{t \in \text{clos}(\text{parent}(\varphi_i(p)))} \Sigma^t} (\varphi_{j*}^{-1}\varphi_{i*}\sigma_r)(\psi_s)\sigma_s(v). \quad (13)$$

Equation (13) illustrates the two key points needed to compute the constraint matrix  $I_c^u$ :

- (1) If  $p \in S$  and  $\text{parent}(p) \neq \emptyset$ , then functionals in  $W^u$  associated with  $p$  are linear combinations of the functionals associated with points in  $\text{clos}(\text{parent}(p))$ . If any of the points in that set has a parent, then we can iteratively apply  $\text{clos} \circ \text{parent}$  to find  $p$ 's *anchor points*, whose functionals will be in the global basis  $W^c$ . This lets us compute the sparsity pattern of  $I_c^u$ .
- (2) The matrix that interpolates to  $\Sigma^p$  from its anchor points' functionals has entries of the form  $(\varphi_{j*}^{-1}\varphi_{i*}\sigma_r)(\psi_s)$  for  $\sigma_r \in \hat{S}$  and shape function  $\psi_s \in P(\hat{K})$ . This lets us compute entries in  $I_c^u$ .

Without further information, entries in  $I_c^u$  must be computed by evaluating transferred functionals of the form  $\varphi_{j*}^{-1}\varphi_{i*}\sigma$  for any non-conformally adjacent cells  $K_i$  and  $K_j$ . In practice, however, non-conformal meshes are usually generated by some predefined set of mesh refinement rules. These rules can be encoded in a small non-conformal mesh that we call the *reference tree*  $\hat{T}$ . For a mesh created by red-green refinement (Fig. 11), for example, every non-conformal transfer map  $\varphi_j^{-1} \circ \varphi_i$  is like mapping one of the edges of the coarse cell  $(a, b, c)$  to one of the refined edges  $(e, f)$ . Due to symmetry, all we have to evaluate are the transferred functionals for  $(\varphi_j^{-1} \circ \varphi_i) \sim (b \mapsto e)$  and  $(\varphi_j^{-1} \circ \varphi_i) \sim (b \mapsto f)$ , which can then be copied into the correct locations in  $I_c^u$ .

#### 4. THE DMPLEXTREE INTERFACE

Support for non-conformal meshes in DMPlex is available in the latest release of PETSc (v3.6), and full documentation can be found online. In this section we introduce the most important components of the interface, starting with the highest-level methods that require the least intervention from the user, and descending into some of the finer controls available to experts.

In Section 3.2, we described how the existence of a predefined refinement pattern, encoded in a reference tree  $\hat{T}$ , can enable DMPlex to compute the constraint matrix  $I_c^u$  more efficiently. The reference tree is also represent by a DMPlex that is assigned to the target mesh (Ex. 2). Reference tree

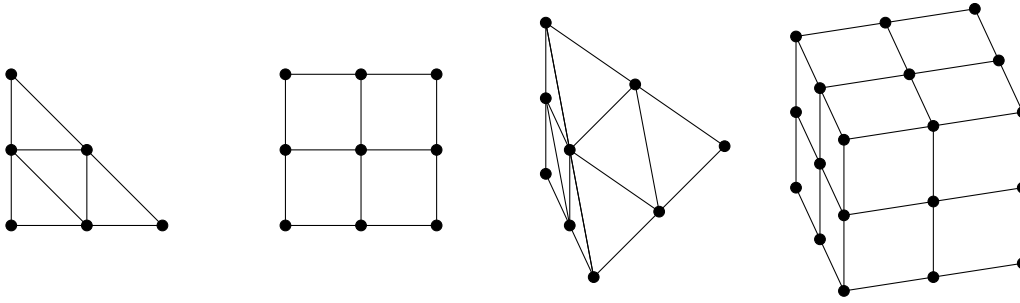


Fig. 12. The refinement patterns for the reference trees created by `DMPlexCreateDefaultReferenceTree()`. The reference trees themselves also contain the original coarse cells.

implementations for isotropic refinement on simplices and hypercubes for  $d = 1, 2, 3$  are provided by PETSc (Fig. 12).

---

**EXAMPLE 2:** Creating a simplicial mesh `dm` and setting the reference tree

---

```

1 MPI_Comm      comm = PETSC_COMM_WORLD;
2 PetscBool    isSimplicial = PETSC_TRUE;
3 DM           dm, refTree;
4 PetscSection parentSection;
5 PetscInt     *parents, *childIDs;

/* Create a DMPlex, using, e.g., DMPlexCreateFromDAG() */
6 DMPlexCreate... (comm, ..., &dm);
/* Create a reference tree that describes the type of non-conformal interfaces in the
   mesh */
7 DMGetDimension(dm, &dim);
8 DMPlexCreateDefaultReferenceTree(comm, dim, isSimplicial, &refTree);
9 DMPlexSetReferenceTree(dm, refTree);
/* dm retains a reference to refTree, this reference can be destroyed */
10 DMDestroy(&refTree);

```

---

One can create a conformal DMPlex mesh from just the cone maps (`DMPlexCreateFromDAG()`), and DMPlex can infer the support maps: likewise, one can create a non-conformal mesh from just the parent maps. In Ex. 3, we demonstrate setting up the parent maps for the simple non-conformal mesh in Fig. 7, assuming that the red-green refinement in Fig. 11 is used as a reference tree.

A DM can encompass not only a mesh, but also the fields discretized on it, using a common interface for both finite element and finite volume methods. In Ex. 4, we set a standard Lagrange  $\mathbb{P}_1(\hat{K})$  finite element on a mesh.

With the reference tree (`DMPlexSetReferenceTree()`), the parent maps (`DMPlexSetTree()`), and the finite element (`DMSetField()`), PETSc will:

- determine the size of the global vector space (the size of  $W^c$  in Eq. (8)),
- compute the constraint matrix  $I_c^u$  from point constraints (Eq. (13)),
- apply  $I_c^u$  when getting the local form of a vector (Ex. 1, line 6), so that the local form represent the vector evaluated at the unconstrained functionals  $W^u$  (Eq. (7)), and `DMPlexVecGetClosure()` gets the vector evaluated at the element functionals  $\Sigma_i$  (Eq. (3)),
- apply  $I_c^{uT}$  when combining local residuals into a global residual (Ex. 1, line 23),

**EXAMPLE 3:** Setting the parent() maps and child IDs for dm

---

```

/* The figures use symbols for points, but we have to assign numbers to them. We count
   across each stratum, starting at the bottom. */
1 PetscInt    numPoints = 16, c = 5, d = 6, e = 7, delta = 14;
/* c is the parent of each of the children */
2 PetscInt    parents[3] = {c, c, c};
/* Set numbers for the relevant points in the reference tree as well. */
3 PetscInt    bRef = 4, eRef = 7, fRef = 8, deltaRef = 12;
/* the childIDs are the points in the reference tree to which the children are
   analogous. d is to its parent (c) as eRef is to its parent (bRef), so that is its
   childID. */
4 PetscInt    childIDs[3] = {eRef, fRef, deltaRef};
5 PetscSection pSec;
6 MPI_Comm    comm = PetscObjectComm((PetscObject)dm);

7 PetscSectionCreate(comm,&pSec);
8 PetscSectionSetChart(pSec,0,numPoints);
9 PetscSectionSetDof(pSec,d,1);
10 PetscSectionSetDof(pSec,e,1);
11 PetscSectionSetDof(pSec,delta,1);
12 PetscSectionSetUp(pSec);
13 DMPlexSetTree(dm,pSec,parents,childIDs);
14 PetscSectionDestroy(&pSec);

```

---

**EXAMPLE 4:** Adding a finite element to a mesh dm

---

```

/* We are creating a scalar field */
1 PetscInt    numComp = 1;
/* We have a simplicial reference element */
2 PetscBool   isSimplex = PETSC_TRUE;
/* The options prefix, for setting options at runtime: e.g., one can change the
   approximation order with '-my_fe_petscspace_order 2' */
3 const char *prefix = "my_fe.";
/* The quadrature order */
4 PetscInt    qorder = 1;
5 PetscInt    dim;
6 PetscFE     fe;

7 DMGetDimension(dm,&dim);
8 PetscFECreateDefault(dm,dim,numComp,isSimplex,prefix,qorder,&fe);
9 DMSetField(dm,0,(PetscObject) fe);
10 PetscFEDestroy(&fe);

```

---

—transform element matrices by the constraints in **DMPlexMatSetClosure()** to correctly assemble a global system matrix from element matrices.

To create a non-conformal mesh that uses a different refinement pattern than the ones provided by PETSc, the user can create a custom reference tree. Any DMPlex that has had the parent maps set with **DMPlexSetTree()** can serve as a reference tree.

If the user does not provide a finite element, then DMPlex cannot determine for itself the layout of the vector space, and the entries in the constraint matrix  $I_c^u$  cannot be calculated automatically. If the user specifies the number of degrees of freedom associated with each process-local mesh point

(using `DMSetDefaultSection()`) then the tree data can be used to both compute the size of the global vector space and the sparsity pattern of  $I_c^u$ . The user can then fill the entries of  $I_c^u$  manually.

There are also potential uses for intra-mesh constraints between degrees of freedom that do not fit into the hierarchical non-conformal framework that is our focus here. The constraint matrix  $I_c^u$  can be a PETSc Mat of any specification, and can be added to a DM directly with `DMSetDefaultConstraints()`. These constraints are applied at the conclusion of `DMGlobalToLocalEnd()`, which gets the process-local representation of a vector, and the transpose of these constraints are applied at the beginning of `DMLocalToGlobalBegin()`, when the contributions of all processes are summed into a global vector.

## 5. VERIFICATION AND EXAMPLE USAGE

In DMPlex's example program `ex3`,<sup>1</sup> we include a small verification that DMPlex handles non-conformal meshes properly. The example can be run to create simplicial or hypercube meshes with non-conformal interfaces.<sup>23</sup> To test that the finite element computations are handled correctly, we construct a symmetric-gradient Laplacian operator  $E$ ,

$$E(u, v) := \int_{\Omega} \frac{1}{2}(\nabla u + \nabla u^T) : \frac{1}{2}(\nabla v + \nabla v^T) dx, \quad (14)$$

and check whether rigid-body motions are in the null-space of  $E$ . The rigid-body motions will be in the null-space of each element matrix that is computed, but if  $I_c^u$  is incorrect, then they will be summed into the global system matrix incorrectly, and it is very unlikely that they will be in the null-space of the incorrect matrix (Ex. 5).

---

**EXAMPLE 5:** Testing the correctness of an assembled Jacobian for a non-conformal mesh `dm` (abridged from `ex3.c`)

---

```

1 MatNullSpace sp;
2 Vec          local;
3 PetscBool    isNullSpace;

/* This tests that the global system size is determined correctly, and that the
   sparsity pattern for global system matrices is computed correctly */
4 DMCreateMatrix(dm, &E);
5 DMGetLocalVector(dm, &local);
/* This is a finite-element loop within PETSc's SNES library that assembles the
   Jacobian matrices of nonlinear equations: the vector local is needed as a dummy
   argument to represent the current "solution" used to evaluate the Jacobian, which in
   this case is the linear operator in Eq. (14). The variational form needed to compute
   each element's matrix has already been attached to dm. */
6 DMPlexSNESComputeJacobianFEM(dm, local, E, E, NULL);
7 DMPlexCreateRigidBody(dm, &sp);
8 MatNullSpaceTest(sp, E, &isNullSpace);

```

---

<sup>1</sup>`src/dm/impls/plex/examples/tests/ex3.c`: run `make ex3` in that directory to build the example.

<sup>2</sup>The initial intent of our work is merely to allow non-conformal meshes to be represented in DMPlex, not to implement a stand-alone adaptive mesh refinement interface. To test the DMPlexTree interface without relying on external libraries, however, we have written `DMPlexTreeRefineCell()`, which hierarchically refines a single cell of a conformal mesh.

<sup>3</sup>To visualize the non-conformal meshes used, go to the `src/dm/impls/plex/examples/tests/` directory of the PETSc source and run `make ex3; ./ex3 -tree -simplex B -dim D -dm_view vtk:nonconf_B.D.vtk:ASCII_VTK` for  $B \in \{0, 1\}$  and  $D \in \{2, 3\}$ .

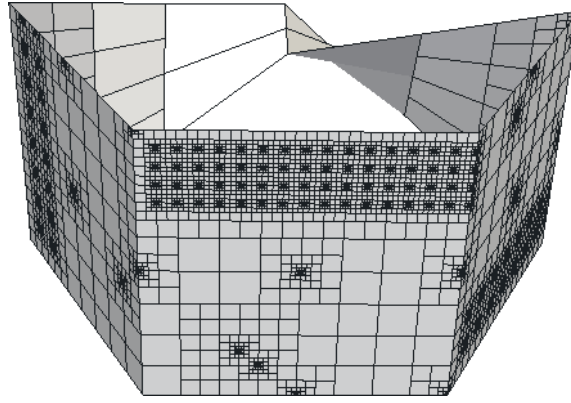


Fig. 13. A Möbius strip mesh, generated in p4est and converted to DMPlex in the example program `p4est_test_plex`.

Example usage outside of PETSc can be found in the p4est library for parallel adaptive mesh refinement [Burstedde et al. 2011], which implements the forest-of-quadtrees and forest-of-octrees paradigms in 2D and 3D. This library is meant to provide data structures only, and comes with no built-in solver or finite element framework. By converting the p4est format into DMPlex (building on the methods described in [Isaac et al. 2015] for efficiently converting p4est’s native format to adjacency-based formats like DMPlex), we make PETSc’s numerical methods more readily available to p4est users. Example programs that perform this conversion are distributed with p4est as `p4est_test_plex` (2D) (Fig. 13) and `p8est_test_plex` (3D). The repository of the p4est library<sup>4</sup> has a “petsc” branch that is compatible with PETSc 3.6.<sup>5</sup>

## 6. OTHER DISCRETIZATIONS

The focus of this work has been  $H^1(\Omega)$ -conforming finite elements. We briefly discuss the way our approach to non-conformal meshes in DMPlex affects other discretizations.

### 6.1. $H^{\text{curl}}(\Omega)$ - and $H^{\text{div}}(\Omega)$ -conforming finite elements

PetscFE does not currently implement the covariant and contravariant Piola transforms that are commonly used by  $H^{\text{curl}}(\Omega)$ - and  $H^{\text{div}}(\Omega)$ -conforming finite elements, but these methods can still be formulated via pullback onto reference elements [Rognes et al. 2009], so future PetscFE implementations of these finite elements are a possibility. The discussion of conformal meshes and non-conformal meshes in this work is still valid for these finite elements, with two small modifications:

— The pullback operations are defined to be

$$\varphi_i^* v := \nabla \varphi_i^T v \circ \varphi_i \quad [\text{covariant}, H^{\text{curl}}(\Omega)], \quad (15)$$

$$\varphi_i^* v := |\det \nabla \varphi_i| \nabla \varphi_i v \circ \varphi_i \quad [\text{contravariant}, H^{\text{div}}(\Omega)]. \quad (16)$$

— The trace space  $P(p)$  for a point  $p \in \hat{S}$  involves not only restricting the function space  $P(\hat{K})$  to the point, but also restricting to the tangential component ( $H^{\text{curl}}$ ) or the normal component ( $H^{\text{div}}$ ).

<sup>4</sup><https://bitbucket.org/cburstedde/p4est/>

<sup>5</sup>To build these examples, run `./configure --with-petsc=$PETSC_DIR` and `make test/p4est_test_plex test/p8est_test_plex`. To view the DMPlex meshes created in these tests, run the examples with the flag `-dm_view vtk:p4est_petsc.vtk:ASCII.VTK`.

The core operation to compute continuity constraints is the transfer of a functional from one element  $K_i$  to its neighbor  $K_j$  and evaluation on a shape function,  $(\varphi_{j*}^{-1}\varphi_{i*}\sigma)(\psi) = \sigma(\varphi_i^*\varphi_j^{-*}\psi)$ . After one verifies that  $\varphi_i^*\varphi_j^{-*} = (\varphi_j^{-1} \circ \varphi_i)^*$  for both pullbacks above, then it must be true that if each child-to-parent map  $\varphi_j^{-1} \circ \varphi_i$  is represented in the reference tree  $\hat{T}$ , then it can be used to compute the entries in the constraint matrix  $I_c^u$ .

## 6.2. The finite volume method

Finite volume methods do not promote the encapsulation of complexity as well as finite element methods. We have formulated our non-conformal mesh extension for finite elements such that, in a typical finite element loop (Ex. 1), the operations performed on each cell in the loop do not depend on whether or not any of the points in the cell's closure is a child or a parent. In a cell-centric approach to the finite volume method, the act of reconstructing centroid values requires determining the neighbors of a cell, which becomes more complex when multiple cells may be on the opposite side of a face (in Fig. 7, e.g., both cells  $B$  and  $C$  are opposite cell  $A$  across edge  $c$ ). While we are currently incorporating non-conformal meshes into the finite volume method as implemented by PetscFV (we expect to finish while this manuscript is in review), the result is likely to be more fragile to user extensions.

One particular aspect that will be counterintuitive to users who worked with finite volume methods on conformal meshes is that a facet can have more than two cells in its support. One often finds in finite volume code constructs of the form “neighbor = (supp[0] == me) ? supp[1] : supp[0],” which are no longer valid. One also has to avoid double-counting fluxes, i.e., computing fluxes on both a parent facet and its children.

Because many unstructured finite volume methods do not care about the shape of cells (i.e., whether they are triangles or quadrilaterals), these issues can be avoided by encoding non-conformal meshes as conformal (though degenerate) ones, as in Fig. 8. In a multiphysics setting, where a finite volume field and a finite element field are involved in a larger system of equations, this approach is not possible.

## 7. DISCUSSION

We have presented an extension to PETSc's DMPlex interface for unstructured meshes so that it can now represent hierarchical non-conformal meshes. Our extension leaves the interface for conformal meshes the same, but adds a tree structure to encode the hierarchy of subsets (children) and supersets (parents). We have shown how, for a wide class of finite elements, by combining this hierarchical information with a reference tree that describes the types of non-conformal interfaces that appear in a mesh, the extra complexity of non-conformal meshes can be hidden, allowing finite element code written for conformal meshes to be applied to them. This extension can already be used to convert p4est forest-of-quadtrees and forest-of-octrees meshes to DMPlex. Work is underway to bring support for the finite volume method up to the level of the finite element method, and future work on the discontinuous Galerkin method is planned.

## 8. ACKNOWLEDGMENTS

We gratefully acknowledge the support of the Intel Parallel Computing Center at the University of Chicago.

## REFERENCES

- Michael Bader, Kaveh Rahnema, and Csaba Vigh. 2012. Memory-efficient sierpinski-order traversals on dynamically adaptive, recursively structured triangular grids. In *Applied Parallel and Scientific Computing*. Springer, 302–312.
- Satish Balay, Shrirang Abhyankar, Mark F. Adams, Jed Brown, Peter Brune, Kris Buschelman, Lisandro Dalcin, Victor Eijkhout, William D. Gropp, Dinesh Kaushik, Matthew G. Knepley, Lois Curfman McInnes, Karl Rupp,

- Barry F. Smith, Stefano Zampini, and Hong Zhang. 2015a. *PETSc Users Manual*. Technical Report ANL-95/11 - Revision 3.6. Argonne National Laboratory.
- Satish Balay, Shrirang Abhyankar, Mark F. Adams, Jed Brown, Peter Brune, Kris Buschelman, Lisandro Dalcin, Victor Eijkhout, William D. Gropp, Dinesh Kaushik, Matthew G. Knepley, Lois Curfman McInnes, Karl Rupp, Barry F. Smith, Stefano Zampini, and Hong Zhang. 2015b. PETSc Web page. <http://www.mcs.anl.gov/petsc>. (2015).
- Carsten Burstedde, Lucas C. Wilcox, and Omar Ghattas. 2011. p4est: Scalable algorithms for parallel adaptive mesh refinement on forests of octrees. *SIAM Journal on Scientific Computing* 33, 3 (2011), 1103–1133.
- Allen Hatcher. 2002. Algebraic Topology. *Cambridge UP, Cambridge* (2002).
- Tobin Isaac, Carsten Burstedde, Lucas C. Wilcox, and Omar Ghattas. 2015. Recursive Algorithms for Distributed Forests of Octrees. *SIAM Journal on Scientific Computing (accepted)* (2015). arXiv:1406.0089.
- Matthew G Knepley and Dmitry A Karpeev. 2009. Mesh algorithms for PDE with Sieve I: Mesh distribution. *Scientific Programming* 17, 3 (2009), 215–230.
- Michael Lange, Matthew G. Knepley, and Gerard J. Gorman. 2015. Flexible, Scalable Mesh and Data Management using PETSc DMPlex. In *EASC2015: Solving Software Challenges for Exascale*. arXiv:1505.04633.
- Marie E. Rognes, Robert C. Kirby, and Anders Logg. 2009. Efficient assembly of H(div) and H(curl) conforming finite elements. *SIAM Journal on Scientific Computing* 31, 6 (2009), 4130–4151.
- Timothy J. Tautges, Ray Meyers, Karl Merkle, Clint Stimpson, and Corey Ernst. 2004. *MOAB: A Mesh-Oriented Database*. SAND2004-1592. Sandia National Laboratories.